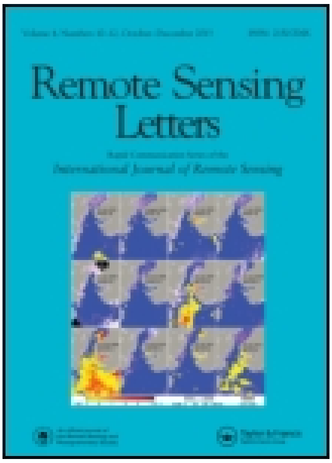

Remote Sensing Letters
Publication details, including instructions for authors and subscription information:
http://www.tandfonline.com/loi/trsl20

Discrete classification approach to land cover and land use change identification based on Landsat image time sequences

Douglas A. Stow[a], Hsiao-Chien Shih[a] & Lloyd L. Coulter[a]
[a] Department of Geography, San Diego State University, San Diego, CA 92182, USA
Published online: 31 Oct 2014.

Remote Sensing Letters, 2014
Vol. 5, No. 10, 922–931, http://dx.doi.org/10.1080/2150704X.2014.976883

Discrete classification approach to land cover and land use change identification based on Landsat image time sequences

Douglas A. Stow*, Hsiao-Chien Shih, and Lloyd L. Coulter

Department of Geography, San Diego State University, San Diego, CA 92182, USA

(*Received 1 August 2014; accepted 10 October 2014*)

Dense multi-temporal stacks of Landsat imagery have most commonly been exploited to identify land cover and land use changes (LCLUC) based on detection of abrupt changes in continuous value spectral indices. In this study, a discrete classification approach to LCLUC identification based on stable training sites is tested on a nine-date, 4-year Landsat-7 ETM + time sequence for a study area in Ghana that is prone to cloud cover. Change to Built cover, as an indication of urban expansion, was identified for over 70% of testing units when a spatial-temporal majority filter that ignored No Data values from clouds, cloud shadows and sensor effects was applied. More important, relatively stable LCLU maps were generated and No Data effects should not limit the potential of the approach for longer-term retrospective analyses or monitoring of LCLUC in cloud-prone regions.

1. Introduction

Recent availability of freely accessible, pre-processed imagery from Thematic Mapper (TM), Enhanced Thematic Mapper Plus (ETM+) and Operational Land Imager (OLI) sensors on Landsat satellites has stimulated the exploitation of moderate-spatial resolution image time sequences (or stacks or series) (Melaas, Friedl, and Zhu 2013; Schneider 2012; Woodcock et al. 2008; Zhu and Woodcock 2014). Such multi-temporal image sequences potentially enable derivation of land surface change information at greater temporal resolutions than in the past, when images had to be purchased, required extensive pre-processing and land cover and land use change (LCLUC) analyses were mostly limited to bi-temporal image analyses.

Multiple approaches to semi-automated LCLUC analysis can be implemented, with the primary choices being distinguished by continuous or discrete data time series analysis, pixel (Yuan et al. 2005) or object-based (Bontemps et al. 2008) classification, and temporal trajectory and post-classification comparison (Liu and Zhou 2004) strategies. The most common approach for dense multi-temporal Landsat image stacks has been the generation of continuous data time sequences of spectral indices to assess vegetation phenology and/or temporal anomalies associated with LCLUC (Melaas, Friedl, and Zhu 2013; Schneider 2012). Schneider (2012) used dense time stacks of Landsat Normalized Difference Vegetation Index (NDVI) data and pixel-based image classifiers to map urbanization in China based on Landsat temporal trajectories. Decision tree classifiers were used to map urban change (as anomalous departures from seasonal trends) by classifying the sub-series (i.e., shorter time intervals than the entire time series) of NDVI values simultaneously with an accuracy greater than 90%, but with a limited temporal precision. We found no published research articles that utilized a discrete classification approach for detecting changes from dense Landsat time stacks.

Our objective is to test a pixel-based, discrete-data, post-classification comparison approach for identifying LCLUC and particularly urbanization, from a noisy time stack of

*Corresponding author. Email: stow@mail.sdsu.edu

Landsat TM/ETM+/OLI data for a study area in southern Ghana during the period late-1999 through late-2003. The area is prone to cloud cover (with associated shadows when cloud cover is patchy), smoke, haze and dust transported by harmattan (dry desert) winds. Along with the Landsat 7 ETM+ scan-line-corrector-off (SLC-off) since April 2003 (Storey, Scaramuzza, and Schmidt 2005), these atmospheric effects result in a Landsat time series that contains many 'no data' pixels. We test an approach based on individual date supervised classification using stable training features and subsequent post-classification comparison to determine whether the classification results are sufficiently stable and spatially and temporally comprehensive to enable subsequent LCLUC identification that would likely entail subsequent application of spatial, temporal and/or logical filtering (Liu and Zhou 2004). We evaluate the reliability and stability in identifying LCLUC (with an emphasis on change to Built cover) based on sample pixels from known features of change and no change.

2. Methodology

2.1. Study area and data

A 7930 km^2 rectangular study area within southern Ghana is shown in Figure 1. The area was selected so as to fall within a single Landsat-7 ETM + path-row 'scene' and represent the variability in LCLU types and biophysical conditions found within Ashanti, Eastern and Greater Accra regions (i.e., states). Six per cent of the area is covered by water, including portions of Lake Volta and the Gulf of Guinea. This equatorial area has a warm, rainy tropical climate with a

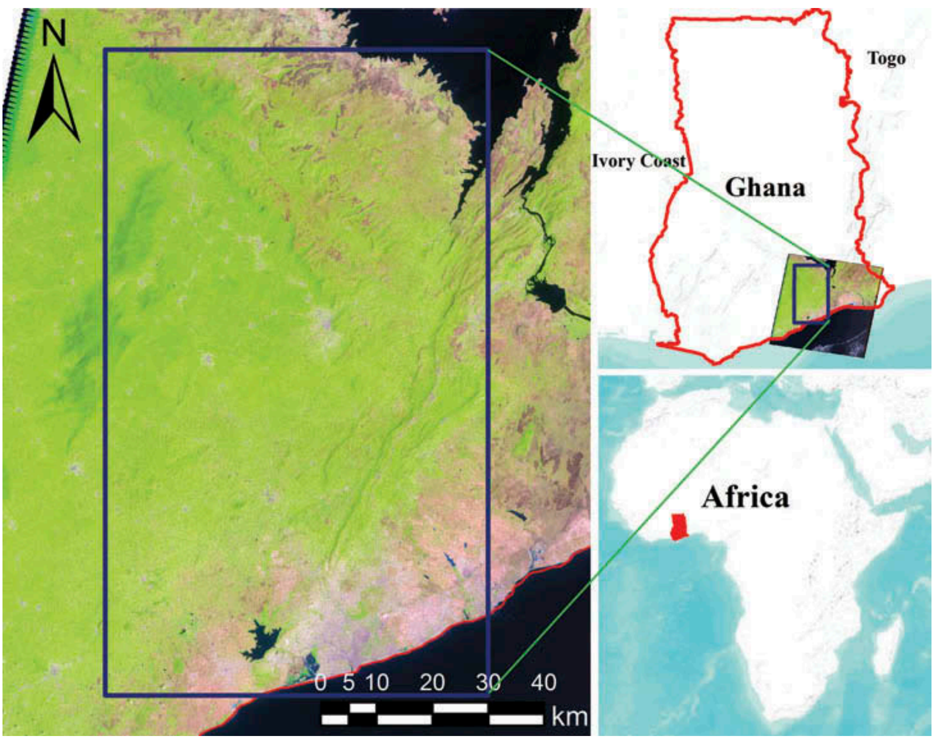

Figure 1. Study area maps with 12 February 2003 Landsat-7 ETM + false colour composite (R = Band 5, G = Band 4, B = Band 3) image subset example. Ghana is outlined and filled in red on upper right and lower right maps, respectively.

Table 1. Listing of dates of Landsat ETM + images utilized for time sequence classification and percentages of No Data, Water and LCLU classes. Percentages after No Data and Water pixels were removed are given in parentheses. NV = Natural Vegetation. Ag/NV = Mixed Agriculture and Natural Vegetation.

Date	No data (%)	Water (%)	Built (%)	NV (%)	Ag/NV (%)
16 November 1999	43.5	6	6.9 (13.7)	17.9 (35.5)	25.6 (50.8)
4 December 2000	31.1	6	6.9 (11.0)	19.5 (31.0)	36.5 (58.0)
22 February 2001	26.0	6	8.7 (12.8)	25.5 (37.5)	33.8 (49.7)
7 December 2001	18.5	6	11.0 (14.6)	26.9 (35.6)	37.6 (49.8)
9 February 2002	16.5	6	10.2 (13.1)	27.1 (35.0)	40.2 (51.9)
10 December 2002	27.0	6	8.7 (13.0)	13.2 (19.7)	45.0 (67.3)
12 February 2003	0.0	6	11.2 (11.9)	35.3 (37.6)	47.5 (50.5)
11 November 2003	35.3	6	7.1 (12.1)	13.9 (23.7)	37.6 (64.2)
13 December 2003	42.7	6	5.9 (11.5)	12.4 (24.3)	32.8 (64.2)

primary dry season from January through April that is more pronounced in the northeastern portion of the study area. Savanna vegetation cover much of the northeast portion near Lake Volta, whereas the rest of the study area was formerly covered by equatorial forests. Small agricultural plots are interspersed amongst natural vegetation. The major city in the study area is Accra, the capital of Ghana and home to over 2.3 million people. Small towns and villages are situated throughout the study area but primarily along or near paved highways and major roads.

Nine Landsat 7 ETM + images captured between 1999 and 2003 were used for this study as listed in Table 1. These terrain-corrected Level 1T Landsat 30-m resolution images were obtained from the Land Processed Data Active Archive Center. These were the only WRS path 193, row 56 images in the 1999 to 2003 time period that were reported to contain less than 33% cloud cover for the entire scene. The images were captured within the drier and more cloud-free November through February period, with exception of a February 2003 image, the only ETM + path 193, row 56 image with less than 10% cloud cover captured between 1999 and 2013. Seven of the nine images were captured before the SLC-off effect occurred. However, Landsat imagery for this study area typically contain some clouds, cloud shadows and haze effects on atmospheric optical quality that can be considered areas of No Data when conducting LCLUC analyses.

Reference data for training LCLU classifiers and evaluating LCLUC trajectories were generated based on 2002 georeferenced QuickBird pan-sharpened multi-spectral data for much of Accra and Google Earth high spatial resolution satellite images covering some urbanized portions of the study in the early 2000s period. A vector map of general LCLU types for 2000 that was produced through on-screen digitizing of Landsat 5 TM imagery by the University of Ghana, Legon was also utilized.

2.2. Image processing

The general approach to LCLUC mapping was to conduct a per-pixel supervised classification for each of the nine ETM + images separately based on training sites considered to be stable throughout the study period, and then analyse the sequence of LCLU maps derived from image classification. No atmospheric correction or radiometric normalization was performed as each image is classified separately (Song et al. 2001). Geometric correction was not necessary for the Level 1T Landsat data, as co-alignment errors between image dates was deemed to be much smaller than the size of the ground resolution element. The strategy is to mask No Data (e.g., clouds, cloud shadows and SLC-off) pixels and then implement relatively simple image classification procedures given the large number of potential image dates in an operational LCLUC mapping scenario.

Normalized difference indices (NDI) were derived from ETM + brightness values based on the equation NDI = $(m-n)/(m + n)$, where the pair (m,n) corresponds to the brightness values for two of the ETM + wavebands. These NDI included: Normalized Difference Vegetation Index (NDVI) (4,3), Normalized Difference Infrared Index (NDII) (4,5), Normalized Difference Blue-Green (NDBG) (1,3), Normalized Difference Green–Red (NDGR) (2,3) and Normalized Difference Red–Blue (NDRB) (3,1). NDI were used as input to image classifiers as they provided greater temporal stability and enhanced class separability compared to spectral brightness values.

Prior to LCLU classification, we classified and masked clouds, cloud shadows, smoke and water bodies in each image. We implemented the thick cloud, shadow and water body removal routine developed by Zhu and Woodcock (2012) that is based on normalized difference image inputs. A mask of these cover types was applied to each image, such that No Data pixels were not subject to classification for that date.

A general LCLU classification scheme was deemed appropriate for the application objectives (LCLUC in relation to rural–urban migration) and the spectral-radiometric characteristics of the Landsat data. The classes are Built, Natural Vegetation (NV) and Agriculture/Natural Vegetation mix (Ag/NV). Built land cover subclasses include low, medium and high density urban. Natural Vegetation consists of four sub-classes: forest, shrub thicket, open shrub with trees and savanna. Three subclasses were used to train on Ag/NV mix: crop/tree mix, crop/grass mix, crops and fallow (bare soil).

Stable training pixels were selected to derive date-specific training data from each of the nine images (Gray and Song 2013). One block training area (between 100 and 500 contiguous pixels) was chosen for each subclass (three for agricultural crops) based on the areas that had not changed from 1999 to 2003 (Reese et al. 2002). Selection of training areas was guided by selection of spectrally and spatially homogeneous areas using an unsupervised classification with 20 cluster classes. The first and last image dates were visually compared to high spatial resolution imagery when coverage was available. The first date of imagery was emphasized for selecting Built training sites, with the assumption that Built cover persist through the study period. For Natural Vegetation, the latter dates were emphasized with the rationale that such areas were undeveloped throughout the study period. Agricultural training sites were selected from the latter two dates, with subsequent cross-checking of the same pixels on the first date to ensure that agricultural development had not already occurred.

Training samples of multi-spectral values and normalized difference indices were extracted for training sites of each sub-class and image date. No Data pixel values (0) were ignored when deriving training statistics (e.g., mean, variance and co-variance). Histograms and statistics were evaluated for the first image date and found to be normally distributed.

A per-pixel maximum likelihood classifier was implemented to generate LCLU maps for each image date. The maximum likelihood classifier was selected because it is relatively robust and readily available routine (for technology transfer purposes) and because fewer training samples are required compared to machine learning classifiers. Having to generate a large number of training pixels would be contradictory to the stable training and discrete classification approach to LCLUC analysis. Inputs to the classifier were the brightness values for Landsat ETM + Band 1 through 5 and also Band 7 and the five normalized difference indices, and related training statistics. The classifier assigned a LCLU class to each unmasked pixel for each image date.

2.3. Validation of LCLU class trajectories

Testing sample units consisting of nine contiguous pixels were extracted from areas of apparent LCLUC (from non-Built to Built) for validation and verification purposes. The units were selected based on visual interpretation of the ETM+, 2002 Quickbird and Google Earth imagery, for locations where high spatial resolution imagery coverage was available for the study period. An emphasis was placed on areas that transitioned to Built cover, since this is the primary type of LCLUC within the study area and period, and the primary change of interest for our broader study of drivers on impacts of LCLUC in Ghana. Thirty (30) Change to Built testing units were selected as reference data for areas that were Ag/NV or NV in the first three dates of imagery and Built some time during the last six image dates. In addition, 60 nine-pixel sampling units were also selected from randomly located No Change areas, 30 for persistent non-Built (Ag/NV or NV) and 30 for persistent Built areas. It was not feasible to visually identify change from NV to (i.e., agricultural expansion) or Ag/NV to NV (i.e., agricultural abandonment) from the limited available high spatial resolution imagery, so no testing units were extracted for this type of transition.

Agreement/disagreement statistics between reference data and Landsat time sequence classification products were based on a combined three-date temporal and nine-pixel spatial majority rule (i.e., majority class of 27 pixels) for each testing unit. The nine contiguous pixel and three contiguous dates were chosen for testing the accuracy of the LCLUC product to account for uncertainty between the product and reference data, and to better represent the precision in identifying LCLUC from a Landsat time series. This meant that the majority class for the nine contiguous pixels for the first three image dates (late-1999 to early-2001) were compared to the majority of the same nine pixels for each of the latter three image dates (2003). Percentage of No Data (cloud, shadow, SLC-off) pixels was also tabulated. To check for false positives (commission errors) in detecting Change to Built, we also examined the 60 No Change testing areas to see if the classification results yielded a majority of Built pixels during the middle three dates (late-2001 to late-2002). The class with the majority of the 27 pixels was determined both for all pixels (including No Data) and with No Data pixels excluded.

3. Results

Frequencies of No Data pixels resulting from clouds, cloud shadows, extreme haze and SLC-off (latter two dates only) for the nine-date sequence of mostly cloud-free ETM + image sequence are portrayed as a map and histogram in Figure 2 and percentages of No Data pixels within each image are listed in Table 1. For the four-year study period, a full range (0–9 dates) of No Data frequencies is observed, with over half of the pixel locations having only two No Data occurrences for the nine image time sequence and 90.0% having four No Data occurrences or fewer. A west to east (and particularly) southwest to northeast trend from higher to lower frequencies of missing data is apparent. This trend follows the general wet to dry precipitation pattern that is also associated with cloud cover trends. Superimposed on this climatic pattern is the pattern associated with the SLC-off effect, where No Data values are greater near the left and right edges of a ETM + scene. Pixels to the left of the subset are closer to the western edge of the scene, which also increases the frequency of No Data pixels in the western portion of the study area. The percentage of No Data pixels ranged from 0.0% for the 12 February 2003 subset to 43.5% for the 16 November 1999 subset, with the median of nine dates at 27.0%.

An example of the LCLU classification map for the cloud-free (12 February 2003) subset is shown in Figure 3. Though detailed reference data for this time period and the

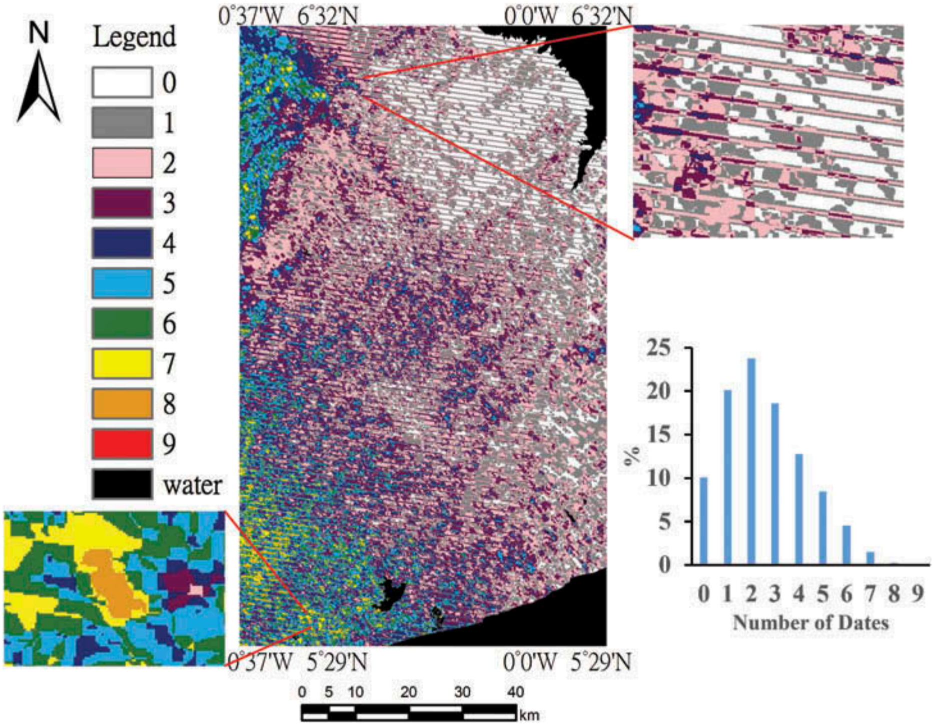

Figure 2. Map depicting number of Landsat ETM + pixels containing No Data values out of a sequence of nine image dates between late-1999 through late-2003. No Data values results from masking of clouds, cloud shadows, severe haze and the ETM + scan-line-corrector-off effect. Histogram (lower right) depicts percentage of pixels in the study area having between 0 and 9 No Data values for the nine most cloud-free dates.

entire study area are limited, the map reasonably portrays the distribution of Built cover, which meets our main objective. This is confirmed by comparison with the 2000 LCLU map, though such comparison also suggests that some areas of mixed agriculture and natural vegetation (Ag/NV) cover were classified as NV (only natural vegetation). LCLU cover percentages shown in Table 1 suggest that the relative proportions of cover types are stable. Stability in classification performance is important if a supervised, date-by-date classification approach to LCLUC time series analysis is to be effective.

Two LCLUC maps emphasizing Change to Built cover from the first three dates (late 1999–early 2001) to the last three dates (2003) of imagery in the nine-date sequence are depicted in Figure 4. Figure 4(*a*) is based on the spatial-temporal majority class (including No Data) for the first and last three-date periods for each pixel, while the map Figure 4(*b*) was derived by excluding No Data values in the majority operation. Clearly, inclusion of No Data values in the individual date classification maps leads to excessive No Data (i.e., no change identification) pixels in the LCLUC map, as a No Data majority for either time period yields No Data for the change identification map. Focusing on Figure 4(*b*), most of the Change to Built pixels (depicted in yellow) are located adjacent to No Change Built areas of Accra and other cities and villages, as would be expected. Some false identification of Change to Built is evident in areas covered by senescent herbaceous savanna vegetation near the shores of Lake Volta. False classification of Built cover in a primarily agricultural area northwest of Accra for the early period resulted in the false change

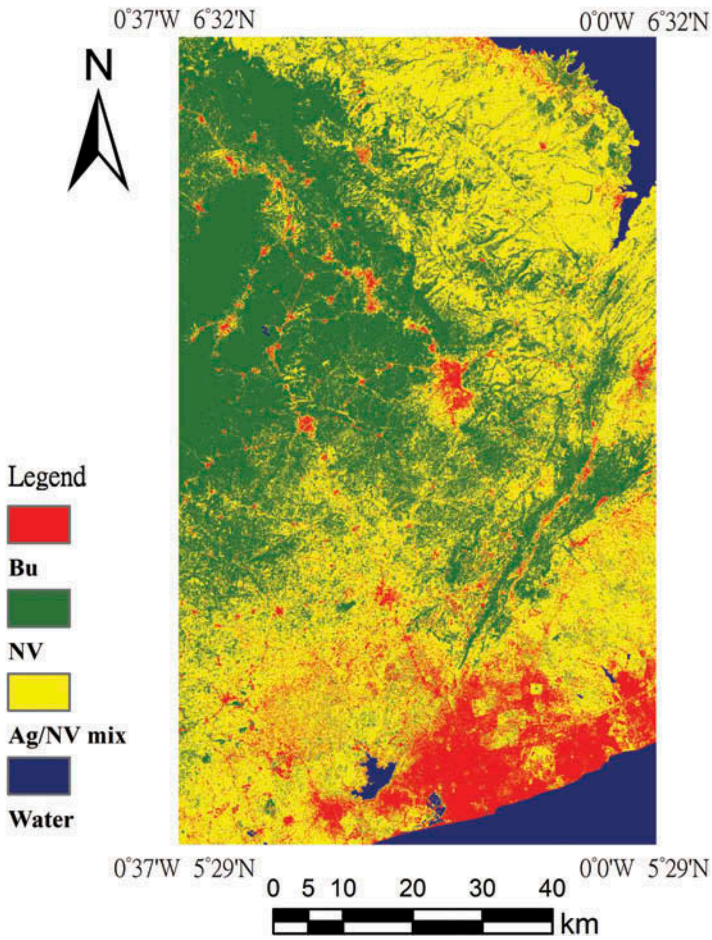

Figure 3. Resultant image classification product depicting general land cover and land use derived from supervised classification of the 12 February 2003 Landsat-7 ETM + subset that is cloud free; this is the only ETM + path 193, row 56 image with less than 10% cloud cover captured between 1999 and 2013.

identification of Built to Non-Built cover for this area (depicted in white). Such errors can be readily removed through a logical filtering operation (i.e., Built land use does not transition to Non-Built in most situations).

Results of the accuracy assessment for 90 nine-pixel testing units are listed in Table 2. Fifteen (50%) of the 30 units determined to represent Change to Built are in agreement when No Data values are included in the space-time majority assessment, with 10% of the units being identified as No Change Built and No Change Non-Built, and 30% No Data as listed in Table 2(a). When No Data pixels are excluded from the majority category assessment, 73.3% of the Change to Built units are in agreement with the Landsat-derived LCLUC map, with 13.3% each of the units being identified as No Change Built and No Change Non-Built as listed in Table 2(b). For the No Change Built and No Change Non-Built testing units, the LCLUC map was in 100% agreement when No Data values are excluded, and 60% and 50% agreement, respectively, when No Data pixels are included in the majority assessment. Thus, no false detection of Change to Built was evident for the 60 No Change test sample units, even though small and spurious examples of false detections

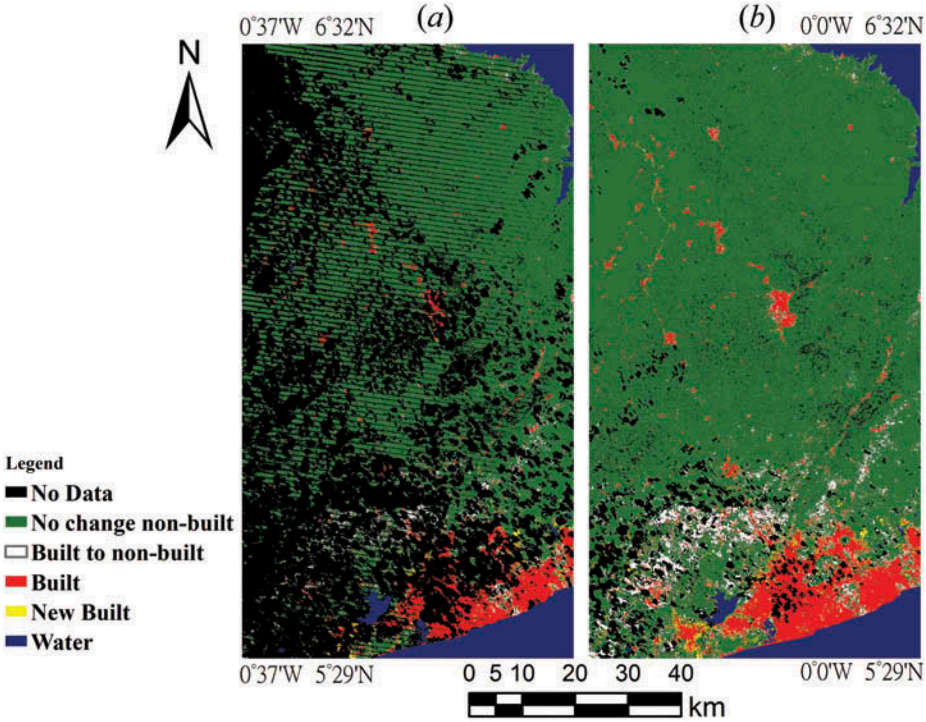

Figure 4. Change to Built and No Change (Built and Non-built) map based on spatial-temporal majority rule, including (*a*) No Data values in majority rule and (*b*) excluding No Data values in majority rule.

Table 2. Agreement–disagreement between reference data test units and LCLUC data from Landsat time sequence classification, (a) including No Data pixels in spatial-temporal majority filtering and (b) excluding No Data pixels in spatial-temporal majority filtering.

		Reference		
		Change to Built	No Change Built	No Change Non-built
(a)				
Classification	Change to Built	15 (50.0%)	0 (0.0%)	0 (0.0%)
	No Change Built	3 (10.0%)	18 (60.0%)	0 (0.0%)
	No Change Non-built	3 (10.0%)	0 (0.0%)	15 (50.0%)
	No Data	9 (30.0%)	12 (40.0%)	15 (50.0%)
	Total	30	30	30
(b)				
Classification	Change to Built	22 (73.3%)	0 (0.0%)	0 (0.0%)
	No Change Built	4 (13.3%)	30 (100.0%)	0 (0.0%)
	No change Non-built	4 (13.3%)	0 (0.0%)	30 (100.0%)
	Total	30	30	30

are apparent in the LCLUC maps in Figure 4. Of the 60 No Change testing units, no false detection of Change to Built for the middle three images resulted. Images from the middle three dates contained a higher proportion of cloud cover and cloud shadows.

4. Discussion and conclusion

The empirical analysis results for the discrete classification approach to identifying LCLUC from a time sequence of Landsat ETM + images that contain clouds, cloud shadows, haze and SLC-off effects are sufficiently promising to warrant further analysis for longer time series. Though these results are certainly specific to the study area and study period, both the amount of cloud cover over the study area and limited amount of LCLUC within the study period provided a challenging test case; the change analysis technique may have greater potential in other study areas and time frames.

As was the case for this study, generating or accessing detailed and precise reference data for assessing the accuracy of LCLUC approaches and products can be challenging and uncertain, particularly for earlier dates of a time sequence. The number and size of testing units were limited because of the general lack of high spatial resolution imagery and other historical reference data, and the limited amount and expansiveness of new Built features from late-1999 to 2003 in the study area. Even so, the Landsat classification results were in agreement with over 70% of the relatively small Change to Built testing units and false detections were generally limited to small spurious pixels and were over a limited extent.

The stable training site approach to image classification yielded relatively stable image classification results over time. The most unstable class is Ag/NV, for areas where fields are fallow and bare soil is exposed. The signature of Built LCLU in Ghana can be influenced by bare soil (roads and clearings around structures), as well as by the iron-oxidized corrugated metal roofs, which are common on residential structures and have a spectral signature similar to bare soil agricultural fields that are high in iron oxides. Training on bare soil agricultural fields is necessary to classify agricultural fields on dates when they are fallow, but can result in Built pixels being classified as Ag/NV; the opposite (fallow agricultural fields being classified as Built) is also an issue. Very little barren land covers the study area and where it does, the patches are small, minimizing the potential for confusion with fallow fields.

Classification instability and No Data gaps in classification results over time necessitate the implementation of spatial, temporal and logical filtering in order to generate reliable LCLUC maps and information from a discrete image time sequence approach. For this study, a combined spatial-temporal majority filter was applied in the examination of agreement–disagreement between the reference data and Landsat image classification sequence. Our follow-on research will examine the utility of multiple spatial and temporal filtering approaches (separately and in combination), as well logical and contextual rule-based filters that can assist in minimizing the effects of classification errors and instabilities (Liu and Zhou 2004).

A discrete classification approach applied to dense Landsat image sequences should be applicable to several LCLUC applications. The approach has the potential to determine not only the type of LCLU transition (i.e., ‘from–to’) but also the time when the transition occurred (or started to occur) for a historical image series. When LCLU mapping is tied to standardized years, such as the beginning of a decade to be concurrent with a decadal census, the approach could be used to determine the LCLU class for missing or noisy pixels captured at the time of the benchmark date. Similarly, hindcasting or forecasting could be performed for a cloud-free image that was captured well before or after the start of the decade. LCLUC information derived from decadal LCLU maps generated from bi-temporal image classification could also be extended to determine the actual date when the LCLUC begin to occur.

The discrete classification approach shows sufficient promise to test it against the more common continuous spectral index tracking and classification approach, which is one of our longer-term objectives. Potential advantages of the discrete approach are: (1) ability to incorporate multiple wavebands, spectral indices and other transform variables, (2) potential for finer temporal resolution in determining date of LCLUC and (3) ability to incorporate stable LCLU training sites rather than training on known locations of specific LCLUC transitions sequences, where the latter is more difficult to identify. Such an evaluation will necessitate use of Landsat Climate Data Records surface reflectance data (LEDAPS processing), which are more critical to successful implementation of spectral index time series tracking than for our discrete multi-temporal image classification approach. The central question to be answered is: since LCLUC analysis inherently involves discrete, categorical data, at what point in the process are continuous Landsat data discretized (classified) to achieve the most reliable product in the most efficient manner?

Acknowledgements

Center for Remote Sensing and Geographic Information Services, University of Ghana, Legon provided 2000 LCLU reference data.

Funding

The study is a component of a project titled 'The Urban Transition in Ghana and Its Relation to Land Cover and Land Use Change Through Analysis of Multi-scale and Multi-temporal Satellite Image Data' funded by the National Aeronautics and Space Administration Interdisciplinary Earth Science Program [grant number G00009708].

References

Bontemps, S., P. Bogaert, N. Titeux, and P. Defourny. 2008. "An Object-Based Change Detection Method Accounting for Temporal Dependences in Time Series with Medium to Coarse Spatial Resolution." *Remote Sensing of Environment* 112: 3181–3191. doi:10.1016/j.rse.2008.03.013.

Gray, J., and C. Song. 2013. "Consistent Classification of Image Time Series with Automatic Adaptive Signature Generalization." *Remote Sensing of Environment* 134: 333–341. doi:10.1016/j.rse.2013.03.022.

Liu, H., and Q. Zhou. 2004. "Accuracy Analysis of Remote Sensing Change Detection by Rule-Based Rationality Evaluation with Post-Classification Comparison." *International Journal of Remote Sensing* 25: 1037–1050. doi:10.1080/0143116031000150004.

Melaas, E. K., M. A. Friedl, and Z. Zhu. 2013. "Detecting Interannual Variation in Deciduous Broadleaf Forest Phenology using Landsat TM/ETM + Data." *Remote Sensing of Environment* 132: 176–185. doi:10.1016/j.rse.2013.01.011.

Reese, H. M., T. M. Lillesand, D. E. Nagel, J. S. Stewart, R. A. Goldmann, T. E. Simmons, J. W. Chipman, and P. A. Tessar. 2002. "Statewide Land Cover Derived from Multiseasonal Landsat TM Data." *A Retrospective of the WISCLAND Project, Remote Sensing of Environment* 82: 224–237. doi:10.1016/S0034-4257(02)00039-1.

Schneider, A. 2012. "Monitoring Land Cover Change in Urban and Peri-Urban Areas Using Dense Time Stacks of Landsat Satellite Data and a Data Mining Approach." *Remote Sensing of Environment* 124: 689–704. doi:10.1016/j.rse.2012.06.006.

Song, C., C. E. Woodcock, K. C. Seto, M. P. Lenney, and S. A. Macomber. 2001. "Classification and Change Detection Using Landsat TM Data: When and How to Correct Atmospheric Effects?" *Remote Sensing of Environment* 75: 230–244. doi:10.1016/S0034-4257(00)00169-3.

Storey, J. P., G. Scaramuzza, and J. B. Schmidt. 2005. "Landsat-7 Scan Line Corrector-Off Gap Filled Product Development." Proceedings of Pecora 16 Global Priorities in Land Remote Sensing, Sioux Falls, SD, October 23–27.

Woodcock, C. E., R. Allen, M. Anderson, A. Belward, R. Bindschadler, W. Cohen, F. Gao, et al. 2008. "Free Access to Landsat Imagery." *Science* 320: 1011. doi:10.1126/science.320.5879.1011a.

Yuan, F., K. E. Sawaya, B. C. Loeffelholz, and M. E. Bauer. 2005. "Land Cover Classification and Change Analysis of the Twin Cities (Minnesota) Metropolitan Area by Multitemporal Landsat Remote Sensing." *Remote Sensing of Environment* 98: 317–328. doi:10.1016/j.rse.2005.08.006.

Zhu, Z., and C. E. Woodcock. 2012. "Object-Based Cloud and Cloud Shadow Detection in Landsat Imagery." *Remote Sensing of Environment* 118: 83–94. doi:10.1016/j.rse.2011.10.028.

Zhu, Z., and C. E. Woodcock. 2014. "Continuous Change Detection and Classification of Land Cover Using All Available Landsat Data." *Remote Sensing of Environment* 144: 152–171. doi:10.1016/j.rse.2014.01.011.